Evaluation of Shunt Model for Simulating Photovoltaic Modules

Yousef Mahmoud ⓘ, *Senior Member, IEEE*, and Weidong Xiao ⓘ, *Senior Member, IEEE*

Abstract—**The complete single-diode model contains one current source, one diode, series, and shunt resistors, which is the most commonly used equivalent circuit for modeling photovoltaic (PV) cell or modules. Simplified models have been developed by eliminating either the shunt resistance or both resistances forming the simplified PV model and the ideal PV model, respectively. While these models have been thoroughly investigated and their pros and cons are well understood in the variety of applications, other simplified formation has not yet comprehensively been investigated or used. This paper investigates the characteristics of the shunt PV model and reveals the feasibility to be utilized for accurately modeling PV modules. A set of equations is derived to parameterize the model relying solely on the information available in manufacturer's datasheets. The model accuracy and its computational time are tested and compared to those of the available models with respect to experimental measurements. The results demonstrate the advantages of the shunt model, which provides a balance between model accuracy and computational time.**

Index Terms—**Maximum power point tracking, photovoltaic, photovoltaic power systems, solar energy.**

I. INTRODUCTION

WITH the increase in solar photovoltaic (PV) electric power penetration to electric grids worldwide, research on PV power systems and their power electronic converters has been growing [1]–[5]. This raises the need for a reliable and effective PV mathematical model, which is valuable for simulation and dynamic analysis [4], [6], [8]. Three main PV models are typically used to model and simulate PV modules as depicted in Fig. 1 [9]–[12].

The complete single-diode PV model composed of a current source, a parallel diode, series, and shunt resistances is considered the most accurate [13]–[16]. However, it relies on a nonlinear transcendental equation, which adds to the model complexity and results in high computational demand for modeling and simulation [17], [18]. The model is typically used when high accuracy is desired [6].

The simplified PV model, shown in Fig. 1(b), neglects the shunt resistance to decrease the complexity [19]. However, it is
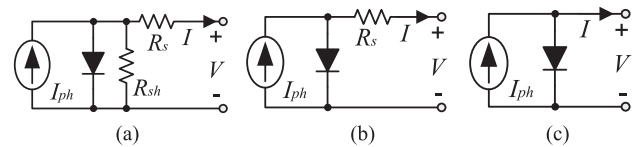
Fig. 1. Prominent equivalent circuits of PV module. (a) Practical model. (b) Simplified model. (c) Ideal model.

still dependent on a transcendental relation that requires high computation. It is usually used to evaluate newly developed MPPT algorithms [20].

The ideal PV model, shown in Fig. 1(c), neglects both resistances and it is considered the simplest model in the literature [21]. It depends on a simple nontranscendental equation, which does not require intense computation [22]. However, the model does not always guarantee accurate output because it has only three degrees of freedom, which are short to represent the maximum power point [23]. The ideal model is chosen mainly for fast simulation or system transient evaluation [24].

In summary, the ideal model is characterized by low computational time, but shows the tradeoff of the lowest accuracy among the three. Meanwhile, if parameterization is proper, the simplified and practical models are distinguished by high accuracy but lack of model efficiency. When a PV array is under homogeneous irradiance and temperature, the total output characteristics can be simulated quickly by using one aggregated model, which shows low computation intensity [25]. However, partially shaded PV systems require simulating hundreds of connected PV models as each PV module might receive different irradiance [26], [27]. This results in an unreasonably high computational time, which increases exponentially with the size of the PV system [28]. Therefore, a mathematical model with the balance of simulation speed and accuracy is demanded for the complex system analysis, such as simulating partially shaded PV systems and developing model-based MPPTs [16], [22], [29].

To address this challenge, a polynomial equation-based PV model was presented to show the balance of accuracy and efficiency [22]. A high performing extraction procedure for single diode parameters was also presented in [30] to ensure higher accuracy for the PV modeling. Similarly, a computational time efficient method that reduces the complexity of parameterization is proposed in [31]. However, the development of model-based MPPTs necessitates a PV model that not only is fast computationally, but also has simplistic features that can produce the inverse model in a closed form [32]. The polynomial PV model, presented in [22], cannot provide this feature
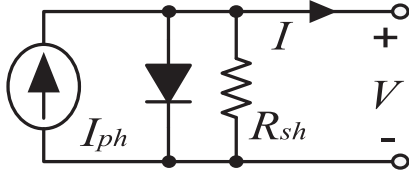
Fig. 2.   Shunt model of a PV module.

in spite of its effectiveness to reduce the computational time. Another PV model, composed of a voltage source, series diode, and series resistance, was developed in [33] for developing model-based MPPT. Although the model provides modeling with sufficient accuracy and speed, its inverse form was not capable to estimate the irradiance accurately without using an iterative solver, which lead to lower power extraction efficiency. Literature review shows that there is still a need to find an unique PV circuit model that shows potential to meet the above requirements. With this goal as a motivation, this paper investigates the characteristics of the shunt PV model and explores its effectiveness and features. It demonstrates that the model can represent PV power output accurately competitive to the practical model, yet requires low computational intensity similar to that of the ideal PV model. These features make the model promising for many applications such as simulating partially shaded PV systems and developing more efficient model-based MPPTs.

The paper starts with the equivalent circuit of the shunt PV model and derives equations for its parameterization in Section II. Evaluation is conducted in Section III to compare with other prominent modeling methods. In Section IV, the computational time of the model is measured and compared to that of the practical model for PV systems of various sizes.

II. SHUNT PV MODEL

The shunt PV model, shown in Fig. 2, consists of a current source, a diode, and a shunt resistance. The shunt resistance provides a new degree of freedom compared to the ideal PV model without affecting its nontranscendental characteristic. The following equation describes the relation between its terminal voltage V and output current I:

$$I = I_{ph} - I_s \times \left[e^{\left(\frac{qV}{N_s KTA} \right)} - 1 \right] - \frac{V}{R_{sh}} \qquad (1)$$

where q is the electron charge, K is the Boltzmann's constant, T is the module temperature, and N_s is the number of series connected PV cells in the PV module. It is important to notice that the I–V characteristics in (1) show a nonimplicit form, similar to the simple ideal model. It can be solved analytically by direct substitution without high computational effort of the numerical or iterative solver. This means that the model is represented in an explicit form of $I = f$ [unlike the existing practical and sim-

plified models which are both represented in an implicit form $I = f(I, V)$].

The shunt model has four degrees of freedom represented by the parameters: the photon current I_{ph}, the saturation current I_s, ideality factor of the diode "A," and the shunt resistance R_{sh}. These are sufficient to reproduce the parameters provided by the manufacturing datasheets without the need for extra measured points.

Beginning with the short-circuit current point and substituting $(0, I_{sc})$ in (1) give

$$I_{pho} = I_{sc} \qquad (2)$$

where I_{pho} is the photon current at the standard test conditions (STC) at which the irradiance and temperature are equal to 1000 W/m^2 and 25°, respectively. Similarly, substituting the open-circuit voltage point $(V_{oc}, 0)$ in (1) produces

$$I_{pho} - I_{rs} \times \left[e^{\frac{qV_{oc}}{N_s KTA}} - 1 \right] - \frac{V_{oc}}{R_{sh}} = 0 \qquad (3)$$

where I_{rs} is the saturation current at STC. Substituting (2) in (3) and rearranging in term of I_{rs} give

$$I_{rs} = \left(I_{sc} - \frac{V_{oc}}{R_{sh}} \right) \Big/ \left[e^{\frac{qV_{oc}}{N_s KTA}} - 1 \right] . \qquad (4)$$

Substituting the operating point at the maximum power (V_m, I_m) in (1) yields

$$I_m = I_{pho} - I_{rs} \times \left[e^{\frac{qV_m}{N_s KTA}} - 1 \right] - \frac{V_m}{R_{sh}} . \qquad (5)$$

Solving (2), (4), with (5) and manipulating result in

$$I_{pho} - I_m - \frac{V_m}{R_{sh}} - \frac{\left(I_{sc} - \frac{V_{oc}}{R_{sh}} \right) \times \left[e^{\frac{qV_m}{N_s KTA}} - 1 \right]}{\left[e^{\frac{qV_{oc}}{N_s KTA}} - 1 \right]} = 0. \qquad (6)$$

Finally, using the implicit information that the power derivative at the maximum power is equal to zero ($dP/dV = 0$) results in

$$0 = I_{pho} - I_{rs} \left[e^{\frac{qV_m}{N_s KTA}} - 1 \right] - \frac{2V_m}{R_{sh}} + \frac{-I_{rs} q V_m}{N_s KTA} e^{\frac{qV_m}{N_s KTA}} \qquad (7)$$

Substituting (1) and (4) in (7) and rearranging produce (8) is shown at the bottom of this page.

Equations (2), (4), (6), and (8) determine the four parameters of the shunt PV model appearing in (1) using the steps summarized in the flowchart depicted in Fig. 2. It starts by estimating the value of the STC photon current I_{pho} using direct substitution in (2). The parameters "A" and R_{sh} are then determined by solving (6) and (8), using any numerical method such as the well-known Newton–Raphson technique. If an iteration results in a nondivergent solution, the initial values of the parameters "A" and R_{sh} should be changed. Once "A" and R_{sh} are estimated, they are substituted in (4) to determine the value of I_{rs}.

$$I_{sc} - \frac{V_m}{R_{sh}} - \frac{\left(I_{sc} - \frac{V_{oc}}{R_{sh}} \right) \times \left(\frac{qV_m}{N_s KTA} \right) \times e^{\frac{qV_m}{N_s KTA}} - \left(I_{sc} - \frac{V_{oc}}{R_{sh}} \right) \times \left[e^{\frac{qV_m}{N_s KTA}} - 1 \right]}{\left[e^{\frac{qV_{oc}}{N_s KTA}} - 1 \right]} = 0 \qquad (8)$$

This article has been accepted for inclusion in a future issue of this journal. Content is final as presented, with the exception of pagination.

MAHMOUD AND XIAO: EVALUATION OF SHUNT MODEL FOR SIMULATING PHOTOVOLTAIC MODULES 3

TABLE I
EXTRACTED PARAMETERS OF THE SHUNT MODEL
FOR THE PV MODULES UNDER STUDY

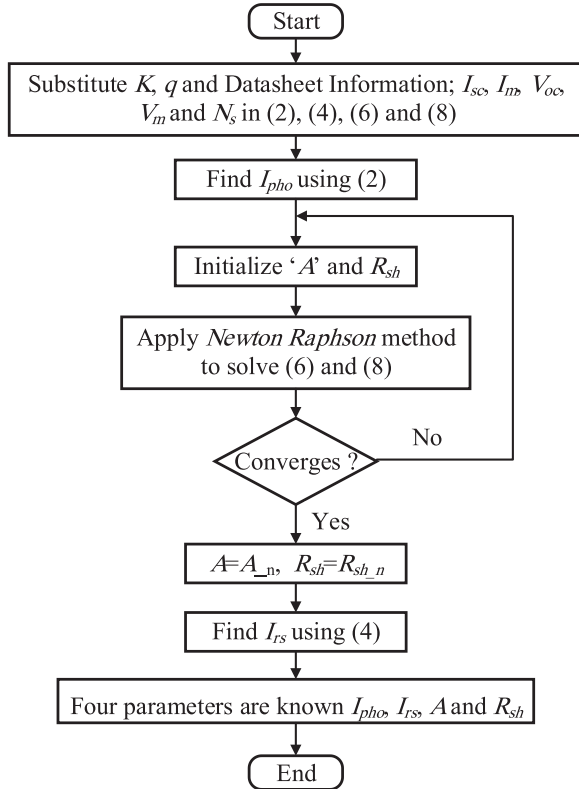| Module Type and Model #		I_{pho}	I_{rs}	A	R_{sh}
MONO	JAM5(l)-72-155	4.94	2.673×10^{-5}	1.949	480.55
	JAM5(l)-72-180	5.44	1.207×10^{-5}	1.864	1027.3
POLY	JAP6-72-250	7.80	2.478×10^{-5}	1.862	1836.2
	NDQ2E3E	7.92	4.573×10^{-5}	1.9105	272.53
THIN	GE-CdTe78	1.23	1.424×10^{-4}	2.6926	9222.7
FILM	NA-E125G5	3.37	4.357×10^{-4}	1.312	182.14

Fig. 3. Flowchart for parameterizing the shunt PV model.

The presented parameterization approach in Fig. 2 is implemented on a range of commercial PV modules of various technologies: monocrystalline, polycrystalline, and thin film. The four parameters resulting from the parameterization (I_{ph}, I_s, A, and R_{sh}) of different PV modules are summarized in Table I. They can be substituted in (1) to plot the current–voltage I–V and power–voltage P–V curves at STC. The curves are shown in Fig. 4(a) and (b). It can be seen that the modeled I–V curves pass precisely through the three items of information given by the manufacturer; (I_{sc}, 0), (0, V_{oc}), and (I_m, V_m). Moreover, the modeled P–V curves pass accurately through the peak power point at its corresponding voltage V_m.

The determined model parameters using the flowchart of Fig. 3 are at STC and, therefore, must be adjusted for the variation of cell temperature and solar irradiance. The photon current I_{pho} is adjusted to the metrological variations, temperature, and irradiance, using (9) [34], where G denotes irradiance (kW/m^2), ΔT is the temperature difference between module temperature and the STC temperature, and α is the current temperature
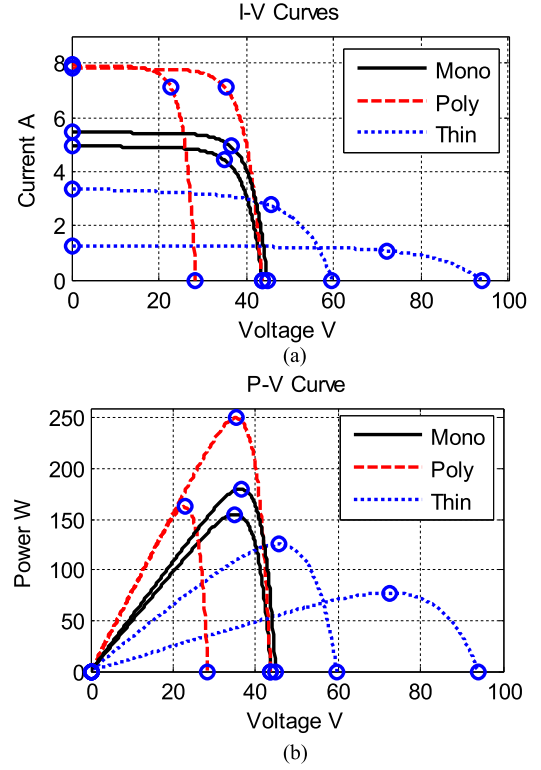

Fig. 4. Modeled characteristic curves for modules in Table I. (a) Current–voltage curves. (b) Power–voltage curves.

coefficient given by the product datasheet [35]

$$I_{ph} = G \left(I_{pho} + \alpha \Delta T \right). \tag{9}$$

The value of the saturation current I_s at any atmospheric conditions can be estimated using (10). A new term is added to improve the accuracy of the model at low irradiances where the value of Y factor can be determined using (11) [22]

$$I_s = \frac{\left(I_{sc} + \alpha \Delta T \right) - V_{oc} - |\beta| \Delta T + Y \ln \left(G/G_o \right) / R_{sh}}{e^{\frac{V_{oc} - |\beta| \Delta T + Y \ln \left(G/G_o \right)}{N_s KTA}} - 1} \tag{10}$$

$$Y = \frac{V_{oc} \left(G_o \right) - V_{oc} \left(G_1 \right)}{\ln \left(\frac{G_1}{G_o} \right)} \tag{11}$$

where $V_{oc} \left(G_1 \right)$ and $V_{oc} \left(G_o \right)$ are the open-circuit voltages at any irradiance G_1 and STC irradiance G_o, respectively.

To summarize, the equations in (9) and (10) are used to adjust the resulted parameters at STC to any irradiance and temperature level. Equation (11) finds the value of the introduced Y factor shown in (10).

III. COMPREHENSIVE EVALUATION OF ACCURACY

The proposed model can accurately pass through the four STC points provided by manufacturer datasheets, as was shown in Fig. 4. This section evaluates the accuracy of the model in the rest points of the curve at different atmospheric conditions. The evaluation is first conducted by comparing the modeled I–V curves using the shunt and existing models at STC to
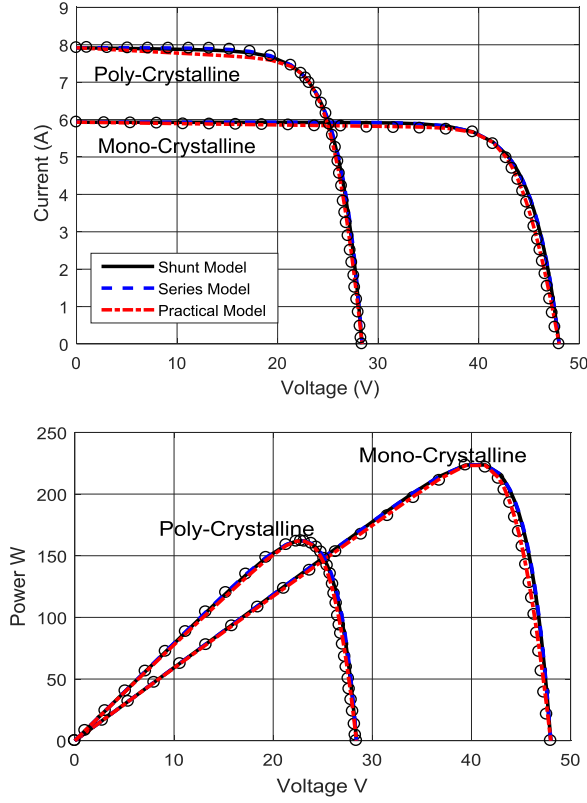
This article has been accepted for inclusion in a future issue of this journal. Content is final as presented, with the exception of pagination.

4   IEEE JOURNAL OF PHOTOVOLTAICS

Fig. 5.   Modeled and measured *I–V* and *P–V* curves for PV modules of different technologies.
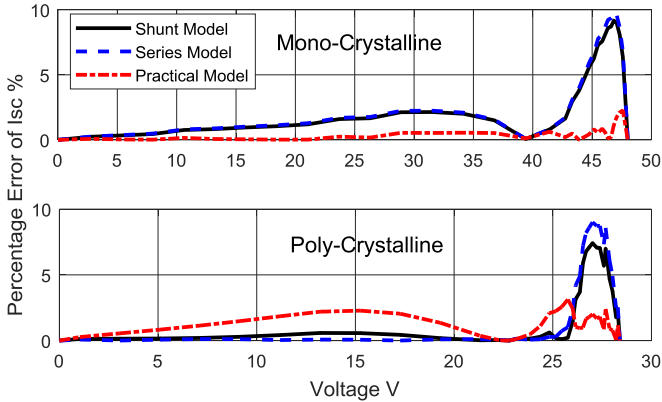

Fig. 6.   Deviations in the practical model and shunt model with respect to measured data.

the measurements provided by the manufacturer's datasheet of Poly Crystalline *NDQ2E3E* and monocrystalline *NA-E125G5* PV modules as illustrated in Fig. 5. The used model for comparison is the most commonly used PV model known as the practical PV model consisting of a single diode, series, and shunt resistances, depicted in Fig. 1(a). The comparison reveals good modeling accuracy. The deviation percentages of the shunt and existing models are depicted also in Fig. 6. As expected, the ideal model has the highest deviation while the practical model has the best accuracy. The shunt PV model is found to have high accuracy similar to that of the practical PV model.

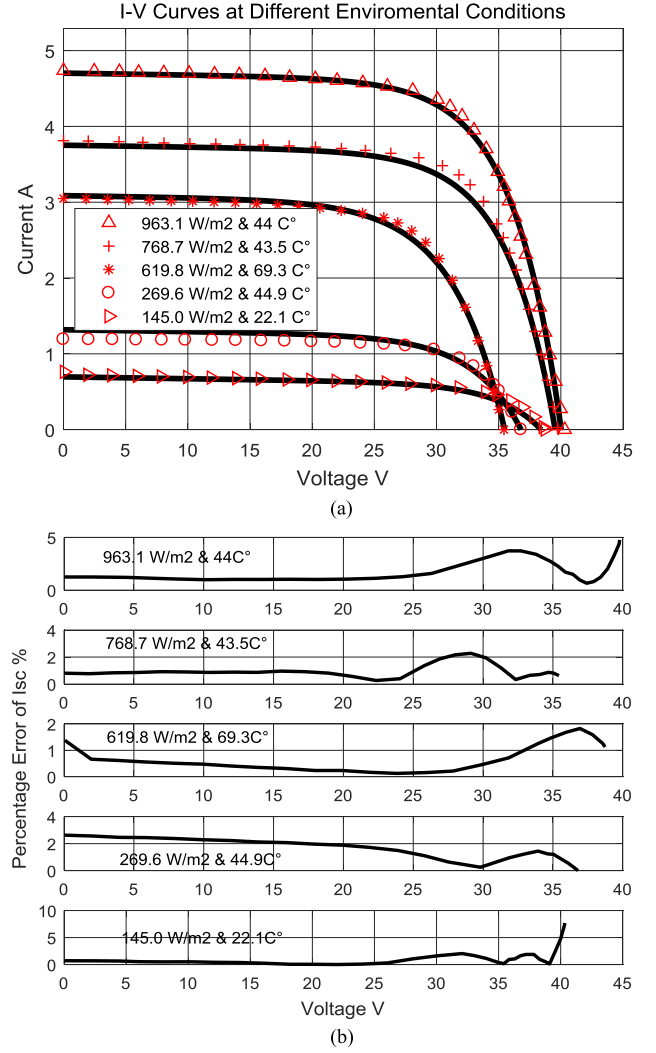A polycrystalline KC167G PV module is modeled also using the shunt PV model and compared to experimental

Fig. 7.   (a) Modeled and experimental *I–V* curves of the PV module under various irradiances and temperatures. (b) Percentage error between the modeled curves and experimental points.

measurements at various atmospheric conditions, as depicted in Fig. 7(a). The comparison demonstrates a good match between the modeled and measured data for the three PV technologies available commercially. The percentage error for all the cases is provided as well in Fig. 7(b). As can be seen, the model successfully matches the experimental data accurately. The percentage error is the ratio between the absolute error and the short-circuit current at STC, which is the maximum current of a PV module.

IV. COMPUTATIONAL TIME COMPARISON

This section evaluates the computational time needed for simulating a PV arrays in MATLAB Simulink using the shunt and the practical PV models. A partially shaded PV system is simulated in MATLAB Simulink using the shunt PV model, and the results are then compared to the practical model. Partially shaded PV systems refer to systems in which not all connected PV modules receive the same irradiance [36]. Monocrystalline JAM5(l)-72-155 PV module is used for the simulation.

The system under study is composed of ten PV strings, each of which has ten series-connected diode-bypassed PV modules.
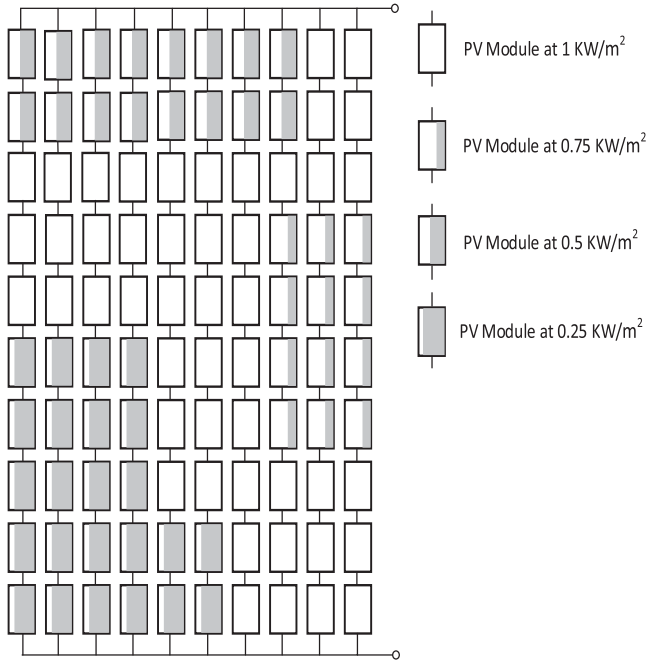
This article has been accepted for inclusion in a future issue of this journal. Content is final as presented, with the exception of pagination.

MAHMOUD AND XIAO: EVALUATION OF SHUNT MODEL FOR SIMULATING PHOTOVOLTAIC MODULES   5

Fig. 8.   Partially shaded PV system under study.

TABLE II
COMPUTATIONAL TIME FOR THE PV SYSTEM UNDER STUDY
USING THE PROPOSED AND PRACTICAL PV MODELS

# of PV strings	Practical Model (s)	Proposed Model (s)	Reduction in Time %
1	2.2150	0.8070	1.40
2	8.6465	3.9500	4.69
3	22.8065	8.4305	14.37
4	48.9465	16.3930	32.55
5	84.3945	28.3675	56.03
6	119.1475	50.3480	68.80
7	182.6900	62.1455	120.54
8	236.0000	94.7000	141.30
9	337.1035	117.5150	219.58
10	419.9420	154.5715	265.37

The shading scenario and irradiance distribution on the PV modules are shown in Fig. 8, where all the modules are working at the temperature of 45°.

Each PV module is represented in Simulink using one PV model. The models are connected in series and parallel to build the system under study. The simulation is built using the shunt PV model and then repeated using the practical PV model.

The simulation is conducted to plot the I–V curves from zero to open-circuit voltage V_{oc}. The computational time is determined using the clock function in MATLAB. First, only one PV string of the system shown in Fig. 8 is simulated (the left-most PV string). The simulation is repeated for two and then three PV strings, until reaching all ten PV strings. The computational times resulting from modeling the system at different sizes are recorded in Table II and also plotted in Fig. 9. As can be seen, the shunt PV model reduces the computational times in comparison with that of the practical PV model. Furthermore, it can be seen that the reduction in the computational time increases with increase in system size. This means that the advantage of
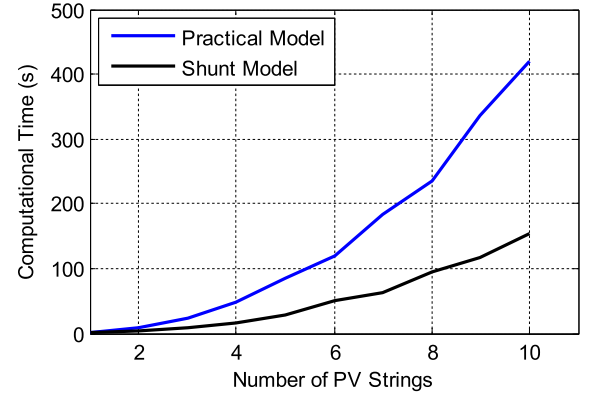

Fig. 9.   Computational time taken to simulate the PV system under study using the shunt and practical models.
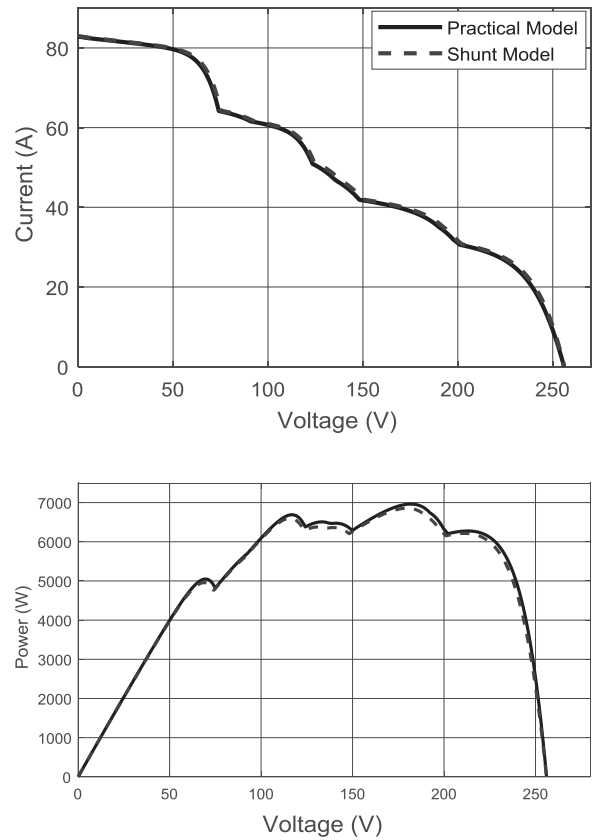

Fig. 10.   Current–voltage and power–voltage curves for the partially shaded PV system under study.

the shunt PV model is amplified, but maintains good accuracy when simulating large PV systems. The accuracy of the shunt PV model is also verified for the partially shaded PV system and compared with that of the practical PV model as depicted in Fig. 10. As seen, they highly match and provide similar accuracy as was tested for homogeneous PV modules earlier in this paper.

V. CONCLUSION

This paper is to investigate the effectiveness of the reduced model, termed as the shunt PV model, which eliminates the series resistance from the conventional single-diode equivalent

circuit. It was indicated that this model relies on the simple non-transcendental equation as the ideal PV model while enhances the accuracy by adding one degree of freedom. The nontranscendental characteristic greatly improves the efficiency in terms of modeling and simulation.

A set of equations is derived to parameterize the model based solely on the information available in manufacturer's datasheets. The model accuracy is tested and compared with those of the available models with respect to experimental measurements for monocrystalline, polycrystalline, and thin-film PV modules, which are commercially available. This demonstrates the benefit of the shunt model, which provides high accuracy similar to that of the practical PV model.

The computational time of the shunt PV model was also explored and compared to that of the practical PV model at different sizes of PV array. The results revealed that the shunt model can simulate significant PV array with greatly reduced computational time. Moreover, it was found that the reduction in computational time increases with the increase in system size, providing clear advantage when modeling and simulating large PV systems. The feature is important for the study of partial shading effect and model-based MPPT.

REFERENCES

[1] M. Chen, K. K. Afridi, S. Chakraborty, and D. J. Perreault, "Multitrack power conversion architecture," *IEEE Trans. Power Electron.*, vol. 32, no. 1, pp. 325–340, Jan. 2017.

[2] R. C. N. Pilawa-Podgurski and D. J. Perreault, "Submodule integrated distributed maximum power point tracking for solar photovoltaic applications," *IEEE Trans. Power Electron.*, vol. 28, no. 6, pp. 2957–2967, Jun. 2013.

[3] Y. Li, Y. Zheng, S. Sheng, B. Scandrett, and B. Lehman, "Modular sub-panel photovoltaic converter system: Analysis and control," in *Proc. IEEE Appl. Power Electron. Conf. Expo.*, 2016, pp. 417–423.

[4] E. I. Batzelis, P. S. Georgilakis, and S. A. Papathanassiou, "Energy models for photovoltaic systems under partial shading conditions: A comprehensive review," *IET Renewable Power Gener.*, vol. 9, pp. 340–349, 2015.

[5] A. Ul-Haq, M. Azhar, Y. Mahmoud, A. Perwaiz, and E. A. Al-Ammar, "Probabilistic modeling of electric vehicle charging pattern associated with residential load for voltage unbalance assessment," *Energies*, vol. 10, 2017, Art. no. 1351.

[6] S. A. Rahman, R. K. Varma, and T. Vanderheide, "Generalised model of a photovoltaic panel," *IET Renewable Power Gener.*, vol. 8, pp. 217–229, 2014.

[7] D. Sera, R. Teodorescu, and P. Rodriguez, "PV panel model based on datasheet values," in *Proc. IEEE Int. Symp. Ind. Electron.*, 2007, pp. 2392–2396.

[8] Y. Mahmoud and E. El-saadany, "Accuracy comparison between Gompertz and polynomial based PV models," in *Proc. IEEE Energy Convers. Congr. Expo.*, 2015, pp. 3278–3281.

[9] M. G. Villalva, J. R. Gazoli, and E. R. Filho, "Comprehensive approach to modeling and simulation of photovoltaic arrays," *IEEE Trans. Power Electron.*, vol. 24, no. 5, pp. 1198–1208, May 2009.

[10] P. Giovanni, R.-P. Carlos Andres, and S. Giovanni, "PV Models," in *Photovoltaic Sources Modeling*. Hoboken, NJ, USA: Wiley-IEEE Press, 2016, p. 208.

[11] W. Xiao, *Photovoltaic Power System: Modelling, Design and Control*. Hoboken, NJ, USA: Wiley-Blackwell, 2017.

[12] S. Lineykin, M. Averbukh, and A. Kuperman, "Issues in modeling amorphous silicon photovoltaic modules by single-diode equivalent circuit," *IEEE Trans. Ind. Electron.*, vol. 61, no. 12, pp. 6785–6793, Dec. 2014.

[13] P. Giovanni, R.-P. Carlos Andres, and S. Giovanni, "Single-diode model parameter identification," in *Photovoltaic Sources Modeling*, Hoboken, NJ, USA: Wiley-IEEE Press, p. 208, 2016.

[14] Y. Mahmoud and E. F. El-Saadany, "Enhanced reconfiguration method for reducing mismatch losses in PV systems," *IEEE J. Photovolt.*, vol. 7, no. 6, pp. 1746–1754, Nov. 2017.

[15] Y. Mahmoud and E. El-Saadany, "Fast reconfiguration algorithm for improving the efficiency of PV systems," in *Proc. 8th Int. Renewable Energy Congr.*, 2017, pp. 1–5.

[16] Y. Mahmoud, "Toward a long-term evaluation of MPPT techniques in PV systems," in *Proc. IEEE 6th Int. Conf. Renewable Energy Res. Appl.*, 2017, pp. 1106–1113.

[17] P. H. Huang, W. Xiao, J. C. H. Peng, and J. L. Kirtley, "Comprehensive parameterization of solar cell: Improved accuracy with simulation efficiency," *IEEE Trans. Ind. Electron.*, vol. 63, no. 3, pp. 1549–1560, Mar. 2016.

[18] E. I. Batzelis, I. A. Routsolias, and S. A. Papathanassiou, "An explicit PV string model based on the Lambert W function and simplified MPP expressions for operation under partial shading," *IEEE Trans. Sustain. Energy*, vol. 5, no. 1, pp. 301–312, Jan. 2014.

[19] I. H. Altas and A. M. Sharaf, "A photovoltaic array simulation model for matlab-simulink GUI environment," in *Proc. Int. Conf. Clean Elect. Power*, 2007, pp. 341–345.

[20] VeeracharyM, "PSIM circuit-oriented simulator model for the nonlinear photovoltaic sources," *IEEE Trans. Aerosp. Electron. Syst.*, vol. 42, no. 2, pp. 735–740, Apr. 2006.

[21] X. Weidong, F. F. Edwin, G. Spagnuolo, and J. Jatskevich, "Efficient approaches for modeling and simulating photovoltaic power systems," *IEEE J. Photovolt.*, vol. 3, no. 1, pp. 500–508, Jan. 2013.

[22] Y. Mahmoud and E. F. El-Saadany, "A photovoltaic model with reduced computational time," *IEEE Trans. Ind. Electron.*, vol. 62, no. 6, pp. 3534–3544, Jun. 2015.

[23] K. Ishaque and Z. Salam, "An improved modeling method to determine the model parameters of photovoltaic (PV) modules using differential evolution (DE)," *Solar Energy*, vol. 85, pp. 2349–2359, 2011.

[24] T. Yun Tiam, D. S. Kirschen, and N. Jenkins, "A model of PV generation suitable for stability analysis," *IEEE Trans. Energy Convers.*, vol. 19, no. 4, pp. 748–755, Dec. 2004.

[25] W. Xiao, F. F. Edwin, G. Spaguolo, and J. Jatskevich, "Efficient approaches for modeling and simulating photovoltaic power systems," *IEEE J. Photovolt.*, vol. 3, no. 1, pp. 500–508, Jan. 2013.

[26] J. R. Louis, S. Shanmugham, K. Gunasekar, N. R. Atla, and K. Murugesan, "Effective utilisation and efficient maximum power extraction in partially shaded photovoltaic systems using minimum-distance-average-based clustering algorithm," *IET Renewable Power Gener.*, vol. 10, pp. 319–326, 2016.

[27] S. Kolesnik *et al.*, "Solar irradiation independent expression for photovoltaic generator maximum power line," *IEEE J. Photovolt.*, vol. 7, no. 5, pp. 1416–1420, Sep. 2017.

[28] Y. Mahmoud and A. Ulhaq, "Computational time quantification of the single diode PV models," in *Proc. 8th Int. Renewable Energy Congr.*, 2017, pp. 1–5.

[29] Y. Mahmoud, "Enhancing the modeling and efficiency of photovoltaic systems," *UWSpace*, 2016.

[30] A. Laudani, F. Riganti Fulginei, and A. Salvini, "High performing extraction procedure for the one-diode model of a photovoltaic panel from experimental I–V curves by using reduced forms," *Solar Energy*, vol. 103, pp. 316–326, 2014.

[31] L. H. I. Lim, Z. Ye, J. Ye, D. Yang, and H. Du, "A Linear identification of diode models from single *I–V* characteristics of PV panels," *IEEE Trans. Ind. Electron.*, vol. 62, no. 7, pp. 4181–4193, Jul. 2015.

[32] L. Cristaldi, M. Faifer, M. Rossi, and S. Toscani, "An improved model-based maximum power point tracker for photovoltaic panels," *IEEE Trans. Instrum. Meas.*, vol. 63, no. 1, pp. 63–71, Jan. 2014.

[33] L. Cristaldi, M. Faifer, M. Rossi, and S. Toscani, "An improved model-based maximum power point tracker for photovoltaic panels," *IEEE Trans. Instrum. Meas.*, vol. 63, no. 1, pp. 63–71, Jan. 2014.

[34] B. C. Babu and S. Gurjar, "A novel simplified two-diode model of photovoltaic (PV) module," *IEEE J. Photovolt.*, vol. 4, no. 4, pp. 1156–1161, Jul. 2014.

[35] S. A. Rahman, R. K. Varma, and T. Vanderheide, "Generalised model of a photovoltaic panel," *IET Renewable Power Gener.*, vol. 8, pp. 217–229, 2014.

[36] H. Patel and V. Agarwal, "Maximum power point tracking scheme for PV systems operating under partially shaded conditions," *IEEE Trans. Ind. Electron.*, vol. 55, no. 4, pp. 1689–1698, Apr. 2008.

Authors' photographs and biographies not available at the time of publication.